Standardised Framework to Study the Influence of Left Atrial RF Catheter Ablation Parameters on Permanent Lesion Formation

Marta Nuñez-Garcia[1(✉)], David Andreu[2], Marta Male[1], Francisco Alarcon[2], Lluís Mont[2], Constantine Butakoff[1], and Oscar Camara[1]

[1] PhySense, DTIC, Universitat Pompeu Fabra, Barcelona, Spain
marta.nunez@upf.edu
[2] Arrhythmia Section, Cardiology Department,
Thorax Institute, Hospital Clínic and IDIBAPS
(Institut d'Investigacions Biomèdiques August Pi i Sunyer), Barcelona, Spain

Abstract. Radiofrequency ablation is a common procedure to treat atrial fibrillation, where the objective is to electrically isolate some regions of the myocardium from others to avoid the transmission of abnormal electrical signals. This is done with a catheter by delivering an RF signal in the targeted regions. Ideally, the signal will create a permanent lesion that would prevent the reappearance of the abnormal electrical signals and therefore terminate AF. There are many parameters involved in the process and naturally in its success. In this paper we present a framework for comparing RF ablation related parameters such as power of the signal, contact force, temperature and impedance with permanent and effective lesion formation. In order to do that we propose to use a standardised unfold map that allows us to directly compare atria with different shapes at different time-points and with different types of information. We tested the method in 8 real cases showing that it facilitates the analysis and comparison of the ablation related parameters with the outcome of the procedure.

Keywords: Left atrium · Radiofrequency catheter ablation · Contact Force · Pulmonary vein isolation · Unfold map

1 Introduction

Atrial fibrillation (AF) triggers are mainly located inside pulmonary veins (PV) [9]. Radiofrequency (RF) PV isolation (PVI) is the most frequent procedure to treat AF [5] by electrically isolating the veins to avoid the transmission of the abnormal electrical signals. The procedure consists in delivering RF energy (typically 30–40 W, 500 kHz) over the tip of a therapy electrophysiology catheter during a certain time across the perimeter of the (typically) four PV. According to Ganesan et al. [7] the long-term success rate ranges from 53.1% with a singe procedure to almost 80% with multiple procedures.

T. Mansi et al. (Eds.): STACOM 2016, LNCS 10124, pp. 96–105, 2017.
DOI: 10.1007/978-3-319-52718-5_11

One of the reasons for this low success rate is the incomplete isolation of the PV due to punctual ablation and the presence of gaps in the lesion (scar or fibrous tissue). Several authors [8,13], have investigated the influence of these anatomical gaps in the recurrence rate of AF. Clearly, incorrect RF ablation (e.g. when the catheter does not touch the LA wall) is a reason for incomplete PV isolation but also other involved parameters can favour the non formation of an effective lesion causing AF recurrence. Parameters related to the delivery of the RF energy such as power of the signal, contact force (CF) [14], temperature or impedance drop may play an important role.

The objective of this study is to investigate the influence of ablation-related parameters on the scar formation around the PVs assessed by a post ablation Late Gadolinium Enhancement (LGE) Cardiovascular Magnetic Resonance (CMR) study. Recent studies have reported the capability of identifying RF ablation lesions in the LA in a 3 months post ablation LGE-CMR study [12], and even to identify lesion gaps in the PV circumference ablation line [1,4]. The task is challenging due to several reasons: during the ablation parameters are recorded at discrete locations (points, coordinates) and a method is needed to merge the information about the LA shape (previously extracted to help guiding the catheter) and the recorded points; additionally, there is LA remodelling due to the ablation procedure and to AF itself [11] and therefore it is difficult to directly compare different atrial shapes; LA segmentation is complicated due to insufficient image resolution to capture thin atrial wall and the segmented LA shapes may appear even more different than they actually are due to segmentation errors.

Trying to overcome these complications several alternative representations of the LA have been proposed. For example, Karim et al. [10] implemented a surface flattening method where one of the clinical applications was to display and compare the unfolded electroanatomical map (endocardial voltage) obtained from mapping systems with the unfolded LGE-CMR map. However, the generated maps are patient-specific and the method does not allow direct comparison between different patients. Therefore, we propose to use the standardised unfold map of the LA defined in [16] that allows us to represent in the same reference system the LA tissue information obtained from the LGE-CMR study and the ablation parameters sampled during the procedure. Having this standard representation we can locally or globally correlate all the parameters involved in the ablation with the scar formation. In addition, we can directly compare results from different patients and investigate the existence of optimal values.

2 Method

The complete framework has four main stages, each of which is explained next. A complete scheme can be seen in Fig. 1.

1. Acquisition of RF-ablation Related Parameters.

In order to integrate the parameters of the RF ablation in a common space the first step is to obtain a representation of the LA shape. Previous to the

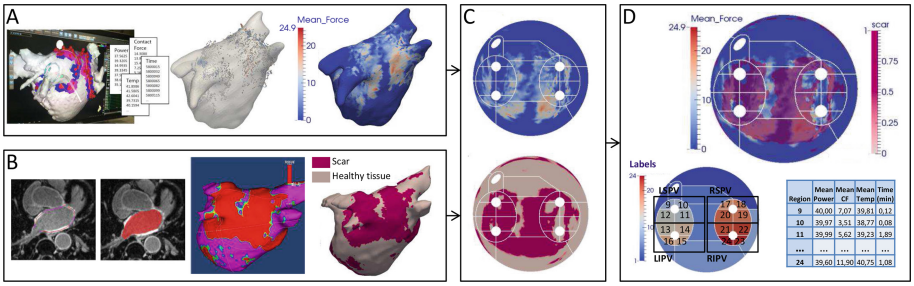

Fig. 1. Complete framework. A. Extraction of the pre-ablation atrial shape and projection of the RF-ablation related parameters (automatically recorded during the ablation and saved in text files (the numbers shown here are unimportant)). In the figure, contact force is shown. B. Extraction of the post-ablation atrial shape and LA wall tissue characterisation: binary classification into either scar or healthy tissue (gaps would be classified as healthy tissue). C. Standardised unfold map of the LA shapes. D. Regional analysis and comparison of the two standardised unfold maps. The upper disk shows the two maps superimposed and the table shows results from the numerical analysis per region (this is an example and the numbers are irrelevant). In the small disk it can be seen the regional division of the LA.

ablation procedure and with the aim of helping guiding the catheter all patients undergo an image study (Computed Tomography (CT) or CMR). The anatomical information is obtained by delineating the LA shape followed by some pre-process (smooth and mesh correction basically) in order to eliminate artefacts due to imaging. This pre-process reduces the potential differences between the two acquisition methods used. During the intervention the mesh is imported into the navigation system and aligned with the current view by rigid registration (rotation and translation). Using the registration matrix it is possible to realign the original mesh and the recorded points afterwards. In the proposed framework this alignment is done by calculating the inverse transformation and applying it to the ablation-related points.

During the ablation the following parameters are saved into the system with a sampling period of 17 ms: position of the catheter tip, power, contact force, temperature and impedance. All this information is projected onto the LA mesh as follows: for each ablation-related sample we find its closest point (vertex) in the mesh. It is noticeable that several ablation-related points may lie on the same LA mesh point. In that situation information is accumulated in the corresponding vertex. Accordingly, vertices of the LA mesh without projected ablation-related points have an assigned value of 0 and are not used in the numerical analysis. The output of this stage is a LA mesh showing the pre-ablation LA anatomy with that information projected (see Fig. 1A).

2. Tissue Characterization of the Post Ablated LA.

Delayed-enhancement CMR images of patients that underwent ablation therapy are typically acquired some months after the procedure in order to assess its success. The regular clinical practice at Hospital Clínic (Barcelona) is to perform the CMR study 3 months after the ablation. From these images, the shape of the LA is extracted by manual segmentation of the LA wall. Binary tissue classification (scar or healthy) is then performed according to the method presented in [3]: Local Image Intensity Ratio (IIR) is calculated as the ratio between the pixel and the mean blood pool intensities. The authors established thresholds based on healthy volunteers and post-ablation patients: an $IIR \leq 1.20$ identifies normal atrial tissue, and an $IIR > 1.32$ identifies dense scarring (see Fig. 1B).

3. Standardised Unfold Map (SUM).

A standardised unfold map (SUM) was proposed in [16] and its main steps are:

1. Mesh standardisation: the PVs and the left atrial appendage (LAA) are semi-automatically clipped. The algorithm requires to manually place a seed close to the ending point of each PV and the LAA. After that, the PVs and LAA are automatically clipped at a distance of the ostium that can be set by the user. Also the mitral valve (MV) is automatically clipped using the information of the placed seeds. We decided to clip the LAA because it is not directly related to PVI. It is important to note that it can extremely vary between different subjects and therefore with that decision we minimise its influence in the following steps.
2. Surface registration of the template where the regions were defined to the standardised atrium resulting from the previous step. This is done by a non-rigid registration based on currents [6] after an initial affine registration.
3. Projection of the registered template to a disk: the MV is mapped to the boundary of the disk and the PV and LAA holes are mapped to predefined holes within the disk.

The resulting disk is a parcellated 2D standard representation of the LA that permits the comparison of the pre- and post-ablated atria that, it is important to remember, have different shapes. In addition, the parcellation of the disk permits performing regional analysis. Finally, representing atria in a 2D map favours fast interpretability and visualisation of the data.

4. Analysis and Comparison of the Ablation and Scar SUMs.

The output of the previous step is a pair of SUMs for each patient: one with ablation-related parameters (i.e. power, contact force, temperature and impedance) and the other one with binary scar segmentation. Let us name these maps *ablation-SUM* and *scar-SUM*. For comparing these two maps we propose the following:

1. Use the parcellation provided by the SUM to evaluate RF-ablation related parameters in each region of the *ablation-SUM*. As we are interested in evaluating the success of PVI we focus in regions representing the surroundings of

each PV. For each vein, its surroundings are divided in four quadrants, thus 16 regions are analysed. We compute the mean and total values of power, contact force and temperature in each SUM region.
2. Localise gaps in the *scar-SUM*. For doing this we follow a strategy similar to the one we recently presented in [8]: we define the *isolating path* as the scar-path that encircles a PV with the minimum amount of gap. We then identify the regions of the SUM where a gap is present. In this study we do not consider the relative amount of gap, only if there is a gap or not. If the gap is less than 10% of the isolating path is ignored.
3. Correlate the information about the gaps (yes/no) with the ablation parameters in all regions: mean and total power, contact force and temperature. With regard to the impedance it is interesting to analyse the impedance drop. In this initial version of the framework we project all the samples to the LA mesh loosing the time reference. We need to take into account the particular temporal instant in order to be able of analysing impedance drops. This could be done complementing the framework adding temporal information but it was left to future work.

Ultimate objective is then to find differences regarding the parameters between regions with and without gaps.

3 Experiments and Results

We applied the proposed method to 8 real cases. The RF catheter used was the Thermocool SmartTouch[1] and the ablation information was acquired with CARTO (See footnote 1). Anatomical information was incorporated from pre-interventional CT or CMR images and the LA shape was extracted from the DICOM images using a research software (ADAS[2]) or CartoMERGE in the case of CT images. The number of ablation-related samples in our data was $98,821 \pm 3,302$ samples. As mentioned before the sampling rate for automatically acquiring these samples was 17 ms, which explains the high number of recorded points. On the other hand, regarding the *scar-SUM*, manual segmentations of the LA wall surface were extracted also using tha ADAS software and tissue classification was performed according to [3] as explained in Sect. 2. For the generation of the SUMs we decided to keep a PV and LAA length of 3 mm in all the cases. The complete framework (pre-processing, mapping and post-processing) was coded in Python using the VTK library. We also used reMESH [2] for correcting mesh imperfections.

Figure 2 and Table 1 show the SUMs generated for one patient and its numerical analysis. The power of the signal was not studied since the recommended power (40 W) was used for all cases. Nevertheless, we found that the mean value is slightly inferior because there are growing and decreasing slopes when passing from 0 W to 40 W and vice versa. With relation to the temperature it can be seen that it is

[1] Biosense Webster Inc, Diamond Bar, CA.
[2] ADAS, Galgo Medical SL. Barcelona, Spain.

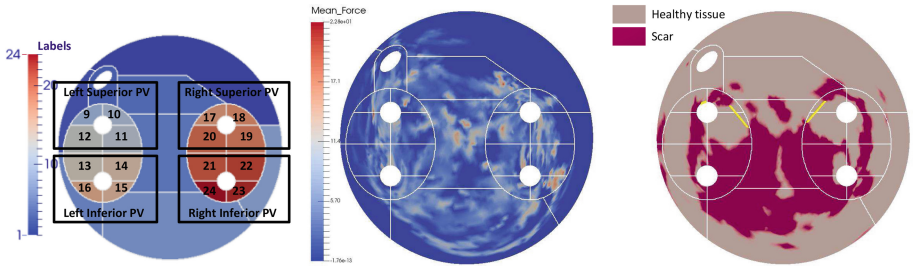

Fig. 2. Example of the 2 SUMs generated for one patient. From left to right: template with region labels; *ablation-SUM* showing in this case the information about contact force; *scar-SUM* showing the segmented scar (magenta) and the detected gaps (yellow). (Color figure online)

Table 1. Some results from the numerical analysis of the example in Fig. 2.

Region	Mean power (W)	Mean contact force (g)	Mean temperature (°C)	Mean time (min)	Gap?
9	37,56	5,29	41,98	2,60	Too small
10	39,32	3,85	42,14	5,05	**Yes**
11	34,99	9,18	41,37	1,12	**Yes**
12	38,49	7,40	41,53	2,41	No
13	39,33	6,10	42,02	0,36	No
14	36,79	3,61	42,74	1,33	No
15	36,17	5,64	41,30	2,17	No
16	36,65	4,87	40,01	0,17	No
17	37,56	4,73	41,57	1,12	**Yes**
18	39,93	6,42	42,12	1,28	No
19	38,66	7,36	41,49	3,25	No
20	35,83	6,76	41,68	3,15	**Yes**
21	39,96	4,22	42,41	2,23	No
22	38,77	6,87	41,92	2,17	No
23	35,13	9,46	40,16	1,37	No
24	39,88	4,47	42,45	0,33	No

Table 2. Numerical analysis results: comparison between regions with and without gap. Shown is the mean ± standard error of power, contact force, temperature, number of CARTO samples and time.

	Power (W)	Force (g)	Temperature (°C)	# CARTO samples	Time (min)
No gap	34.74 ± 1.88	7.82 ± 1.00	39.55 ± 0.94	5035.09 ± 1566.39	1.43 ± 0.44
Gap	34.95 ± 1.34	8.01 ± 0.80	39.35 ± 0.67	7550.80 ± 1857.57	2.14 ± 0.53

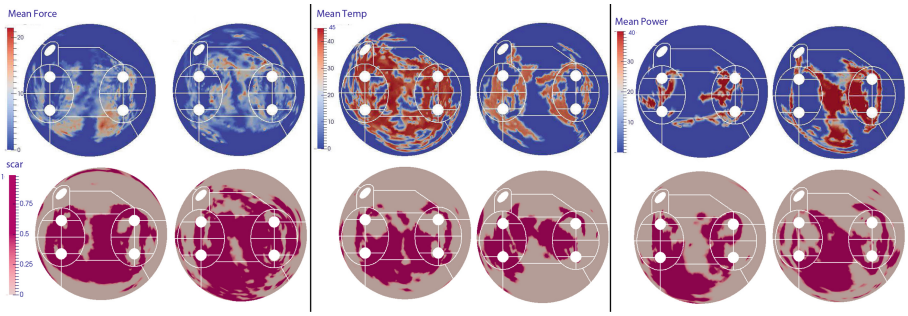

Fig. 3. Examples of pair of SUMs generated: the first row shows *ablation-SUM* and the second row their corresponding *scar-SUM* (each column is a different patient). Regarding the ablation-SUMs examples of contact force, temperature and power are shown.

significantly lower than the typically target temperature (i.e. 50–55 °C). This is due to the fact that the ablation was done with an irrigated catheter (in order to induce a deeper lesion) which is a type of cooled tip ablation [15,17].

In the example shown in Fig. 2, it can be observed that there are two gaps: one in the left superior PV (LSPV) and the other one in the right superior PV (RSPV). Results in Table 1 suggest that the gap in region 10 can be due to low CF even though the ablation time is quite high. We could also hypothesise that the gap in region 11 corresponds to an area insufficiently ablated (see *ablation-SUM* in that region). If we compare regions 17 and 18 we can see that the two regions were ablated during a similar period of time but in region 17 the mean CF and mean power were lower than in region 18. This fact could explain why we see a gap in region 17 and not in region 18. Likewise, if we compare regions 19 and 20 that were also ablated during a similar period of time, we observe again that the mean CF and mean power are lower in the region where there is a gap (20). However, we observe that in other regions good scar patterns were obtained with lower CF, power and in less time. Examples of efficient ablations can be seen in regions 13, 16 and 18 where a good scar pattern was created in a short period of time (see Fig. 2).

We compared the numerical analysis of all patients trying to find common patterns relating the parameters and the presence or absence of anatomical gaps but statistically significant differences were not found (see Table 2). We also analysed the influence of the ablation time: we investigated whether it is more effective to ablate during a shorter period of time with a higher contact force or with lower contact force during a longer period of time but there was not any consistent pattern. Even more, unexpectedly, we found that regions with gaps were ablated (in average) much time and with a higher CF (Fig. 3).

4 Discussion and Conclusions

We have presented a framework to analyse the influence of RF-ablation parameters in the formation of a permanent lesion that would, ideally, terminate AF. For that, we decided to use a standardised unfold map that permits directly compare atria with different shapes and with different kind of information. Our aim was to identify optimal values of the parameters but we did not find clear thresholds from our experiments. Some potential reasons are: (1) The dataset is too small for extracting well founded conclusions; (2) The LA wall is very thin and its segmentation is complicated: there are segmentation errors that can affect the results; (3) Patients with AF may have natural fibrosis (not induced by the ablation) that would be classified as scar in the tissue classification process. It would be convenient to perform tissue classification previous to the RF-ablation in order to be able to differentiate between natural and ablation induced fibrosis. For this study we did not have access to the pre-ablation images but we plan to enrich the method by including this information in the future; (4) The objective during the ablation is to have as less gaps as possible and therefore in the data there are not many of them.

For future work we plan to have access to a bigger dataset and improve the segmentation method used. We also plan to automatically analyse the amount of gap in each of the SUM regions and not only its presence or absence. Similarly to what was done in [8], we will investigate if there is correlation between the parameters and a quantitative measure describing the amount of gap in each region.

Acknowledgements. This work was partially supported by the EU FP7 for research, technological development and demonstration under grant agreement VP2HF (no 611823) and by the Spanish Ministry of Economy and Competitiveness (DPI2015-71640-R). The authors would like to thank Catalina Tobon-Gomez, Steven E. Williams and M. Henry Chubb for their valuable help.

References

1. Andreu, D., Gomez-Pulido, F., Calvo, M., Carlosena-Remírez, A., Bisbal, F., Borràs, R., Benito, E., Guasch, E., Prat-Gonzalez, S., Perea, R.J., et al.: Contact force threshold for permanent lesion formation in atrial fibrillation ablation: a cardiac magnetic resonance-based study to detect ablation gaps. Heart Rhythm **13**(1), 37–45 (2016)
2. Attene, M., Falcidieno, B.: Remesh: an interactive environment to edit and repair triangle meshes. In: IEEE International Conference on Shape Modeling and Applications, p. 41 (2006)
3. Benito, E., Carlosena-Remírez, A., Guasch, E., Prat-Gonzalez, S., Perea, R.J., Figueras, R., Borràs, R., Andreu, D., Arbelo, E., Tolosana, J.M., Bisbal, F., Berruezo, A., Brugada, J., Mont, L.: Left atrial fibrosis quantification by late gadolinium enhancement magnetic resonance: a new method to standardize the thresholds for reproducibility. Europace. Epub ahead of print (2016)

4. Bisbal, F., Guiu, E., Cabanas-Grandío, P., Berruezo, A., Prat-Gonzalez, S., Vidal, B., Garrido, C., Andreu, D., Fernandez-Armenta, J., Tolosana, J.M., et al.: Cmr-guided approach to localize and ablate gaps in repeat af ablation procedure. JACC: Cardiovasc. Imaging **7**(7), 653–663 (2014)
5. Calkins, H., Kuck, K.H., Cappato, R., Brugada, J., Camm, A.J., Chen, S.A., Crijns, H.J., Damiano, R.J., Davies, D.W., DiMarco, J., et al.: 2012 HRS/EHRA/ECAS expert consensus statement on catheter and surgical ablation of atrial fibrillation: recommendations for patient selection, procedural techniques, patient management and follow-up, definitions, endpoints, and research trial design. Europace **14**(4), 528–606 (2012)
6. Durrleman, S., Prastawa, M., Charon, N., Korenberg, J.R., Joshi, S., Gerig, G., Trouvé, A.: Morphometry of anatomical shape complexes with dense deformations and sparse parameters. NeuroImage **101**, 35–49 (2014)
7. Ganesan, A.N., Shipp, N.J., Brooks, A.G., Kuklik, P., Lau, D.H., Lim, H.S., Sullivan, T., Roberts-Thomson, K.C., Sanders, P.: Long-term outcomes of catheter ablation of atrial fibrillation: a systematic review and meta-analysis. J. Am. Heart Assoc. **2**(2), e004549 (2013)
8. Nuñez Garcia, M., Tobon-Gomez, C., Rhode, K., Bijnens, B., Camara, O., Butakoff, C.: Quantification of gaps in ablation lesions around the pulmonary veins in delayed enhancement MRI. In: van Assen, H., Bovendeerd, P., Delhaas, T. (eds.) FIMH 2015. LNCS, vol. 9126, pp. 215–222. Springer, Heidelberg (2015). doi:10.1007/978-3-319-20309-6_25
9. Haissaguerre, M., Jaïs, P., Shah, D.C., Takahashi, A., Hocini, M., Quiniou, G., Garrigue, S., Le Mouroux, A., Le Métayer, P., Clémenty, J.: Spontaneous initiation of atrial fibrillation by ectopic beats originating in the pulmonary veins. New Engl. J. Med. **339**(10), 659–666 (1998)
10. Karim, R., Ma, Y., Jang, M., Housden, R.J., Williams, S.E., Chen, Z., Ataollahi, A., Althoefer, K., Rinaldi, C.A., Razavi, R., et al.: Surface flattening of the human left atrium and proof-of-concept clinical applications. Comput. Med. Imaging Graph. **38**(4), 251–266 (2014)
11. Kuppahally, S.S., Akoum, N., Badger, T.J., Burgon, N.S., Haslam, T., Kholmovski, E., Macleod, R., McGann, C., Marrouche, N.F.: Echocardiographic left atrial reverse remodeling after catheter ablation of atrial fibrillation is predicted by pre-ablation delayed enhancement of left atrium by magnetic resonance imaging. Am. Heart J. **160**(5), 877–884 (2010)
12. McGann, C., Kholmovski, E., Blauer, J., Vijayakumar, S., Haslam, T., Cates, J., DiBella, E., Burgon, N., Wilson, B., Alexander, A., et al.: Dark regions of no-reflow on late gadolinium enhancement magnetic resonance imaging result in scar formation after atrial fibrillation ablation. J. Am. Coll. Cardiol. **58**(2), 177–185 (2011)
13. Peters, D.C., Wylie, J.V., Hauser, T.H., Nezafat, R., Han, Y., Woo, J.J., Taclas, J., Kissinger, K.V., Goddu, B., Josephson, M.E., et al.: Recurrence of atrial fibrillation correlates with the extent of post-procedural late gadolinium enhancement: a pilot study. JACC: Cardiovasc. Imaging **2**(3), 308–316 (2009)
14. Shurrab, M., Di Biase, L., Briceno, D.F., Kaoutskaia, A., Haj-Yahia, S., Newman, D., Lashevsky, I., Nakagawa, H., Crystal, E.: Impact of contact force technology on atrial fibrillation ablation: a meta-analysis. J. Am. Heart Assoc. **4**(9), e002476 (2015)
15. Thomas, S.P., Aggarwal, G., Boyd, A.C., Jin, Y., Ross, D.L.: A comparison of open irrigated and non-irrigated tip catheter ablation for pulmonary vein isolation. Europace **6**(4), 330–335 (2004)

16. Tobon-Gomez, C., Zuluaga, M.A., Chubb, H., Williams, S.E., Butakoff, C., Karim, R., Camara, O., Ourselin, S., Rhode, K.: Standardised unfold map of the left atrium: regional definition for multimodal image analysis. J. Cardiovasc. Magn. Reson. **17**(1), 1 (2015)
17. Yamane, T., Jaïs, P., Shah, D.C., Hocini, M., Peng, J.T., Deisenhofer, I., Clémenty, J., Haïssaguerre, M.: Efficacy and safety of an irrigated-tip catheter for the ablation of accessory pathways resistant to conventional radiofrequency ablation. Circulation **102**(21), 2565–2568 (2000)